

Growth of crystalline garnet mixed films, superlattices and multilayers for optical applications via shuttered Combinatorial Pulsed Laser Deposition

Katherine A. Sloyan,^{1*} Timothy C. May-Smith,¹ Michalis Zervas,¹ Robert W. Eason,¹ Steven Huband,² David Walker,² Pamela A. Thomas²

¹Optoelectronics Research Centre, University of Southampton, Southampton SO17 1BJ UK

²Department of Physics, University of Warwick, Coventry CV4 7AL UK

*kas@orc.soton.ac.uk

Abstract: A range of crystalline garnet multilayer structures have been fabricated via multi-beam, multi-target PLD in conjunction with a system of mechanical shutters. Structures grown consisted of alternating Gd₃Ga₅O₁₂ (GGG) and Gd₃Sc₂Ga₃O₁₂ (GSGG) layers on Y₃Al₅O₁₂ (YAG) substrates, with both simple and chirped designs. Distinct layers are observed where layer thickness is around 2 nm or greater, although some layering may also be present at a sub-unit cell level. These structures demonstrate the viability of the shutter technique as a quick, simple fabrication method for a variety of optical multilayer structures.

©2010 Optical Society of America

OCIS codes: (310.1860) Deposition and fabrication; (310.4165) Multilayer design; (310.6845) Thin film devices and applications; (160.4670) Optical materials.

References and links

1. K. A. Sloyan, T. C. May-Smith, R. W. Eason, and J. G. Lunney, "The effect of relative plasma plume delay on the properties of complex oxide films grown by multi-laser, multi-target combinatorial pulsed laser deposition," *Appl. Surf. Sci.* **255**(22), 9066–9070 (2009).
2. M. S. B. Darby, T. C. May-Smith, and R. W. Eason, "Deposition and stoichiometry control of Nd-doped gadolinium gallium garnet thin films by combinatorial pulsed laser deposition using two targets of Nd:Gd₃Ga₅O₁₂ and Ga₂O₃," *Appl. Phys., A Mater. Sci. Process.* **93**(2), 477–481 (2008).
3. R. Gazia, T. C. May-Smith, and R. W. Eason, "Growth of a hybrid garnet crystal multilayer structure by combinatorial pulsed laser deposition," *J. Cryst. Growth* **310**(16), 3848–3853 (2008).
4. T. C. May-Smith, and R. W. Eason, "Comparative growth study of garnet crystal films fabricated by pulsed laser deposition," *J. Cryst. Growth* **308**(2), 382–391 (2007).
5. T. C. May-Smith, D. P. Shepherd, and R. W. Eason, "Growth of a multilayer garnet crystal double-clad waveguide structure by pulsed laser deposition," *Thin Solid Films* **515**(20–21), 7971–7975 (2007).
6. T. C. May-Smith, A. C. Muir, M. S. B. Darby, and R. W. Eason, "Design and performance of a ZnSe tetra-prism for homogeneous substrate heating using a CO₂ laser for pulsed laser deposition experiments," *Appl. Opt.* **47**(11), 1767–1780 (2008).
7. S. Stepanov, "GID_sl on the web" http://sergey.gmca.aps.anl.gov/gid_sl.html
8. M. Y. Chern, C. C. Fang, J. S. Liaw, J. G. Lin, and C. Y. Huang, "Study of ultrathin Y₃Fe₅O₁₂/Gd₃Ga₅O₁₂ superlattices," *Appl. Phys. Lett.* **69**(6), 854–856 (1996).
9. Y. Ishibashi, N. Ohashi, and T. Tsurumi, "Structural refinement of X-ray diffraction profile for artificial superlattices," *Jpn. J. Appl. Phys.* **39**(1), 186–191 (2000).
10. M. D. Craven, P. Waltereit, F. Wu, J. S. Speck, and S. P. DenBaars, "Characterization of a-Plane GaN/(Al,Ga)N Multiple Quantum Wells Grown via Metalorganic Chemical Vapor Deposition," *Jpn. J. Appl. Phys.* **42**(Part 2, No. 3A), 235–238 (2003).
11. L. V. Azaroff, *Elements of X-Ray Crystallography* (McGraw-Hill 1968).
12. T.C. May-Smith, K.A. Sloyan, R. Gazia, R.W. Eason, "Stress Engineering and Optimisation of Thick Garnet Crystal Films Grown by Pulsed Laser Deposition," Manuscript submitted to *Cryst. Growth Des.* September 2010.

1. Introduction

Thin film multilayers are of interest in a wide variety of applications, from microwave devices to photovoltaics. They are used extensively in optics; Bragg reflectors, laser diodes and planar

waveguides and waveguide lasers are just a few examples. While a range of fabrication techniques may be employed to create such structures, many processes can be slow, costly or limited to simple materials, and often require harmful precursors or solvents.

Pulsed Laser Deposition (PLD) compares favorably in many situations; in particular, it is suitable for depositing multi-component materials with complex stoichiometries at potentially high growth rates (up to 10 μm per hour). Combinatorial PLD extends the basic PLD setup to include multiple lasers and targets, increasing the number of controllable growth parameters and making the technique even more versatile. It is already making headway in precision materials engineering; strain and stoichiometry control [1, 2] have already been demonstrated, as has material mixing to obtain specific physical properties [3]. However, investigation into the significant promise for structural engineering (multilayers, graded layers, composite crystals etc.) has only just begun.

Some inter-layer mixing in a multilayer system is unavoidable, due to indiffusion, particulates and the potential for island crystal growth. There hence exists a minimum thickness of growth required to obtain distinct layers. We have fabricated a series of multilayer structures with varying layer thicknesses in order to determine at what point the transition from mixed crystal to distinct layering occurs. Subsequently, we have demonstrated further proof of principle via growth of more sophisticated chirped structures. We have achieved this via a shutter technique that will allow us to exploit the advantages of combinatorial PLD to grow crystalline multilayer structures quickly and easily.

Garnets are excellent laser hosts that have been grown in both single film and multilayer geometries [4,5]. Different garnets can be easily mixed to make films with tailored average properties, such as defined lattice constant or refractive index [3]. $\text{Gd}_3\text{Ga}_5\text{O}_{12}$ (GGG) and $\text{Gd}_3\text{Sc}_2\text{Ga}_3\text{O}_{12}$ (GSGG) are two such garnets; they are known to grow well under the same conditions as both single and mixed layers [1], and hence are ideal as tester materials for multilayer and graded growth.

2. Experimental

The setup used was based on the combinatorial PLD system illustrated by Gazia et al [3], with the addition of mechanical beam shutters (see Fig. 1). UV pulses from two frequency quadrupled, flashlamp-pumped Nd:YAG lasers were incident upon single-crystal targets of undoped GGG and (2 at.%Nd, 0.5 at.% Cr):GSGG. The lasers operated at 10 Hz, with a nominal pulse duration of 5 ns and wavelength of 266 nm. Growth rates could not be measured directly, but are known to be approximately the same for similar spot sizes and fluences [1]. Targets were rotated with a target-substrate distance of ~ 45 mm. Plume-substrate angle of incidence was constant and equal for each case, and growth was carried out in a background O_2 pressure of 4.0×10^{-2} mbar.

Substrates were heated to ~ 700 °C using a raster-scanned CO_2 laser. Due to the unknown emissivity of both the growing films and substrate at high temperatures, temperature values were estimated from a separate calibration involving the melting of high-purity metal foils. The temperature homogeneity across the substrate was not measured directly; however, previous modeling of a setup using such a raster-scanned beam suggested a variation of 11 K over the central 36 mm^2 [6]. While this model was based on a square grid of points rather than the concentric circles of points used in this experiment, this value may be used as a guide. We assume that any small temperature variation across the substrate surface does not significantly affect the films grown.

Mechanical shutters physically blocked beam paths. The system could be operated to obtain bursts of pulses and/or to change relative laser repetition rates. Each shutter consisted of a 0.25 mm thick anodized aluminum blade mounted on a rotary solenoid, with opening and closing triggered via a TTL input signal from a *Thorlabs* SC10 shutter control box. Both control boxes were connected to a single PC, and hence sophisticated control could be achieved via a set of custom *LabView* programs.

Shutters were operated alternately, allowing bursts of pulses to deposit GGG and GSGG sequentially on single crystal (100) orientated $\text{Y}_3\text{Al}_5\text{O}_{12}$ (YAG) substrates of size $10 \times 10 \times 1$

mm. The opening time for each shutter, and hence the number of shots per burst (i.e. thickness of material deposited), was varied for each sample.

Ten multilayer films were grown in total, with the numbers of shots per burst ranging from 5 to 5000 across the range of samples. Total deposition time in all but two cases was 30 minutes, yielding a total film thickness of ~400 nm; the number of layers was hence different for each sample. For the 5000 shot sample, total deposition was 1 hour (~800 nm total thickness) and for the 3500 shot sample, total deposition was 47 minutes (~600 nm). Single-material films of both GGG and GSGG were also grown for comparison. Deposition conditions were the same as those for the multilayer samples, with a total deposition time in each case of 15 minutes. For samples with 5 to 1000 shots per layer, a *Stanford* signal generator programmed by hand was used in place of the PC to trigger the control boxes; all others used the *LabView* programs mentioned above.

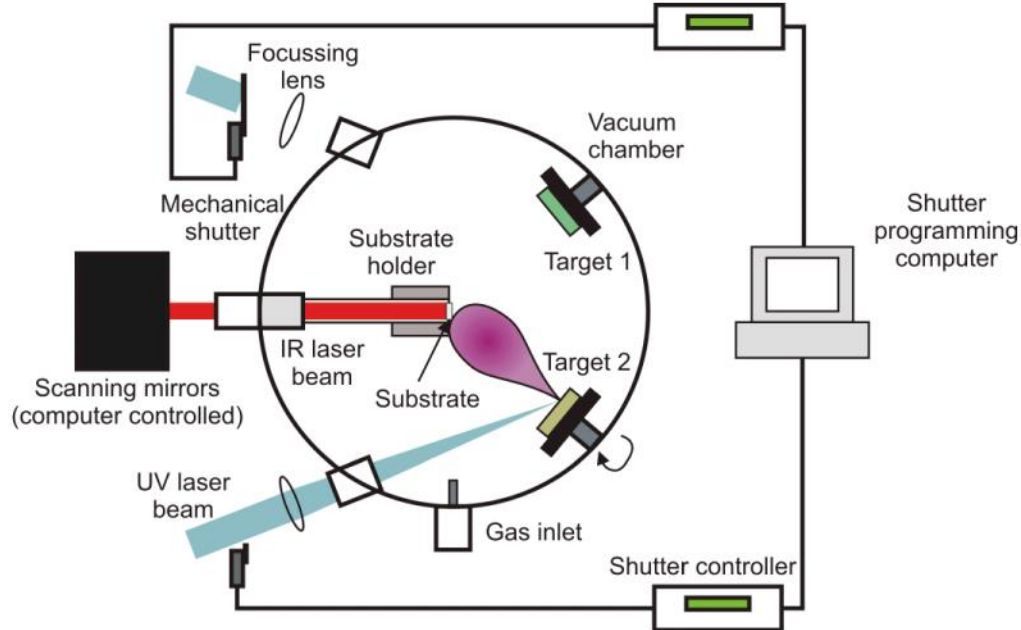


Fig. 1. Combinatorial PLD setup with two lasers and two targets. Shutter 1 is closed, blocking the beam path and preventing ablation, while shutter 2 is open, allowing the laser to ablate Target 2. The sequence of opening and closing of both shutters is set using custom *LabView* programs on a PC, via a shutter control box connected to each unit.

3. Analysis and simulation

Low resolution X-ray diffraction (XRD) was carried out using a *Siemens D5000* powder diffractometer using $\text{Cu K}_{\alpha 1}$ and $\text{Cu K}_{\alpha 2}$ radiation. High-resolution XRD and X-ray reflectometry (XRR) were carried out using a *Panalytical X'Pert Pro* Materials Research Diffractometer equipped with a hybrid monochromator as the incident beam optics, giving pure $\text{Cu K}_{\alpha 1}$ radiation, and a solid state PiXcel detector. For high resolution XRD only, the scans were optimized to the (0 0 4) Bragg peak of the YAG substrate and standard $\theta - 2\theta$ scans measured. In the low resolution case, peak positions were normalized relative to the position of the underlying YAG substrate peak. It should be noted that the instrumental functions of the two diffractometers are different, with low-resolution XRD resulting in spectra with much broader peaks.

XRD scans for the 5 shot to 500 shot cases were simulated using a web-based dynamical X-ray simulation program *GID_sl* [7]. Simulations were convoluted with the instrumental function, with background and noise added after the convolution had been performed. Inputs to the program included layer thickness and layer strain with respect to the substrate,

quantified as the difference between the layer and substrate lattice parameters divided by the substrate lattice parameter da/a . These quantities were varied to fit the positions and heights of the satellite peaks (by fitting overall periodicity and individual layer thicknesses respectively) and position of the 0th order peak respectively. In this way, the experimental values for each simulated sample were approximated. Spectra of the samples with 5 shots and 20 shots per layer consist of an average layer peak without any satellite peaks. To simulate these samples the GGG and GSGG layer were set to have the same lattice constant to fit the data.

Reflectometry measurements were fitted using the *Panalytical* Reflectivity software. Crystal density, layer thickness and roughness were inputs to the program and, as above, were varied in order to achieve the best fit.

4. Results and discussion

All structures grown were crystalline and optically clear. Although single-crystal growth was not explicitly verified, the presence (in the XRD of films grown using a single-target) of only those peaks exhibited by the substrate, and the good match between substrate and film peak shapes, suggests that the films grew in the epitaxial direction. Fitting of XRR data (examples illustrated in Fig. 2) suggests that GGG and GSGG layers have average roughnesses of $2.5 + 0.8/-0.4 \text{ \AA}$ and $4 \text{ \AA} + 2/-3 \text{ \AA}$ respectively, values that compare well to previously reported garnet multilayer PLD films [8]. The (4 0 0) 2θ peak of the underlying YAG substrate (at 29.74°) is clearly seen in all XRD data (see Fig. 3).

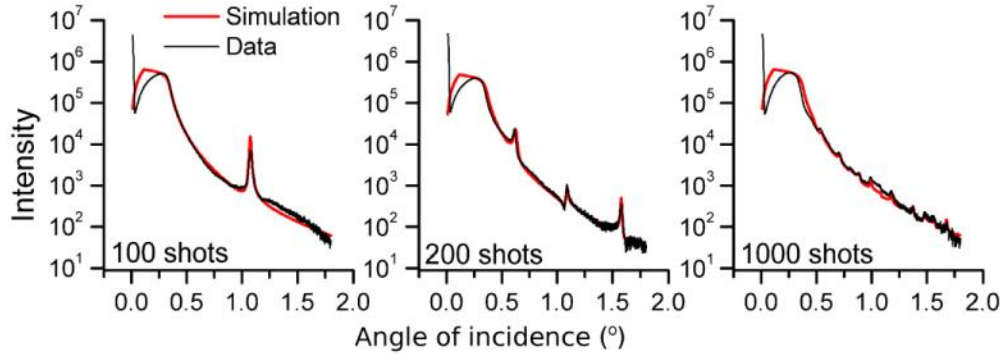


Fig. 2. Examples of x-ray reflectivity measurements (black) and simulated fit (red)

XRD scans show three regimes of behavior: single peak, superlattice and multilayer (see Fig. 3). The samples grown with 5 shots per burst, 500 shots per burst and 5000 shots per burst are examples of each regime respectively. There is also a superlattice-multilayer transition region, with samples of between 500 and 3500 shots per burst showing a combination of superlattice and multilayer behavior.

For the single peak cases (5 shots to 50 shots per burst, ~ 0.1 to 1 nm thickness of material deposited per burst), a strong 2θ peak around 28.4° is observed. This peak position corresponds roughly to the average of the two component peaks, with the spectra consistent with those obtained for fully mixed films [1].

For samples grown with 100 to 1000 shots per burst, satellite peaks can be observed either side of the main central peak. This is consistent with XRD spectra reported in the literature for superlattice structures [8–11], i.e. a periodic array of discrete layers. The intensity of the central peak decreases as number of shots per burst increases from 100 to 1000. From 2500 shots per layer onwards, the central peak is not observed, satellite peaks become less significant and the pattern approaches that of the two component materials. Such a pattern, the two single peaks observed in the 5000 shots per burst case ($\sim 100 \text{ nm}$ per layer), approaches that exhibited by “thick” multilayers ($>1 \text{ \mu m}$ per layer) [3, 5].

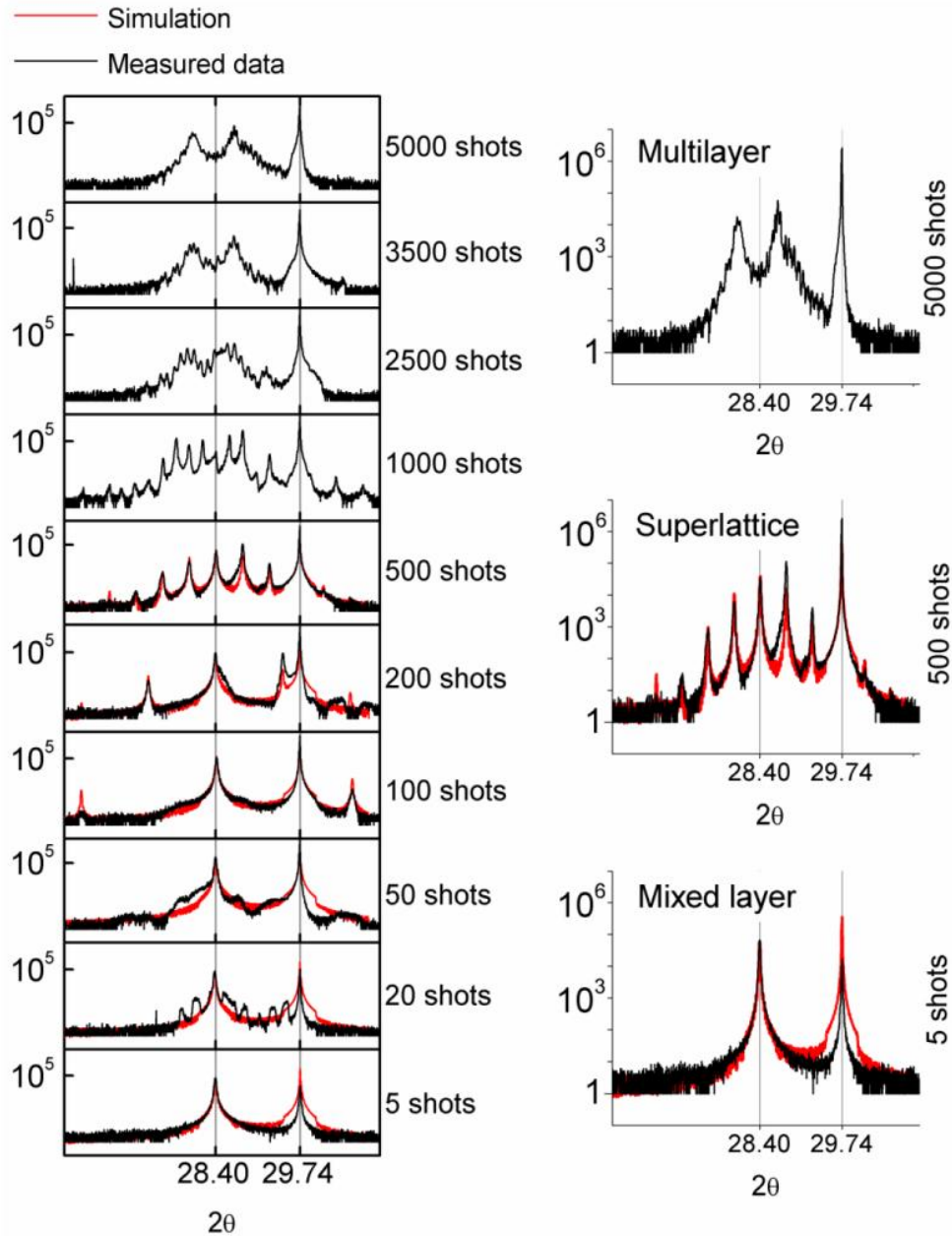


Fig. 3. High resolution logarithmic X-ray diffraction data (black) and simulation (red) for structures fabricated via alternating pulse bursts per target. The number of shots per burst on each target ranges from 5 to 5000 over the range of samples.

The superlattice period P is given by the modified Bragg law [10], shown as Eq. (1):

$$P = \frac{\lambda}{2(\sin \theta_{n+1} - \sin \theta_n)} \quad (1)$$

where θ_n and θ_{n+1} are the positions of the central and first satellite peaks respectively and λ is the X-ray wavelength (Cu $K\alpha_1$ in this case = 1.5406 Å). The values obtained for the films grown are illustrated in Table 1; average thickness of growth per shot is estimated to be ~0.02 nm. A slight drop in growth rate was observed for the 2500 shots per layer case; this is likely

due to target damage following extensive ablation. Single-target 2θ values were somewhat different from literature values: 28.08° for GSGG and 28.60° for GGG, corresponding to lattice parameters of 1.270 and 1.247 nm respectively. This is thought to be the result of a compositional deficiency of gallium, known to occur for PLD of Ga-containing garnets, as well as residual stress in the lattice.

The central peak positions observed do not correspond exactly to the mid point between the GGG and GSGG peak positions, due to slight differences in the growth rates of GGG and GSGG. Layer thickness values were obtained by fitting XRR peaks in the 100, 200 and 1000 shot cases (see Fig. 2), and suggest that the ratio of GSGG to GGG is approximately 1:1.2. This is not unreasonable, given that growth rates were not optimized.

The fitting of XRD data gives further indication of strain and growth rates (see Table 1). Growth per shot values are in good agreement with those measured. Calculated GGG da/a decreases by around 15% over the 100 to 500 shots cases towards the single-material value of 0.039, suggesting that strain marginally decreases; this change has not, however, been examined experimentally.

Table 1. Information about growth rates and layer quality obtained from superlattice samples

Shots/ layer	Measured parameters		Simulated parameters			
	Superlattice period (nm)	Growth/ shot (nm)	Superlattice period (nm)	Growth / shot (nm)	GGG da/a	GSGG da/a
5	-	-	0.22	0.022	0.046	0.046
20	-	-	0.98	0.025	0.047	0.047
50	-	-	2.18	0.022	0.034	0.058
100	4.2	0.021	4.24	0.021	0.034	0.058
200	8.5	0.021	8.54	0.021	0.035	0.058
500	21	0.021	21.5	0.022	0.039	0.058
1000	41	0.021	-	-	-	-
2500	84	0.017	-	-	-	-

PLD-grown films, including those described in this paper, typically exist in a strained state as a result of a number of factors. Laser fluence, thermal expansion mismatch and lattice mismatch all influence film strain, which leads to deformation of the lattice and a corresponding shift in measured XRD peak position. Lattice mismatch, for example, relaxes via dislocations introduced into the lattice as film thickness increases, not fully relaxing until thickness is of the order of microns [12]. Before this, strain due to lattice mismatch leads to an out-of-plane distortion via Poisson's Law. Modeling of films described here can offer some insight: it may be the case that fewer dislocations are introduced when superlattice layers are thinner, given the modeled change in GGG da/a . However, the effect of the different sources of stress in combination has not been fully investigated and hence there may be an unquantified shift in the XRD data and subsequent analysis. Despite this, the overall conclusions remain unaffected.

An anomalous XRD 2θ peak around 30.5° can be seen in the 50 and 200 shot cases. A number of overlaying peaks are also observed in the 20 shot case, and peak broadening in the 50 shot case. The cause of these anomalies has not been determined. However, they are inconsistent with both modeling and low-resolution XRD, and are hence unlikely to be due to the overall multilayer structure.

In general, we see evidence of layering in structures where deposition thickness per pulse burst is 2 nm or more, but mixed-crystal behavior where this thickness is 1 nm or less, i.e. less than a unit cell. The fact that we see evidence of layering right down to the unit cell level suggests that the effect of interdiffusion (even at substrate temperatures of $\sim 700^\circ\text{C}$) and any island growth may not be significant at this scale.

It may, however, be the case that layering is present even at thicknesses below one unit cell. XRD simulations of the 50 shot case (layer thickness ~ 1 nm) show that this single-peak pattern would be practically observed even for a layered material; similarly, XRR simulation suggests that a peak at around 2° incident angle would be expected for a layered structure, but

such a peak would not be discernable from noise in the current setup. The garnet crystal structure, containing 8 planes within the unit cell, is complex enough to allow the possibility of sub-unit cell layering. Similarly, although errors are relatively large due to difficulties in curve fitting, roughness values obtained lie below half a unit cell, and hence roughness is likely not high enough to completely remove layer definition at this scale.

This potential for layering must be considered in any application where such length scales are significant, and in the context of growing “true” multilayer and graded structures, simultaneous deposition (i.e. maximum of 1 shot alternating) is recommended if a mixed layer is desired. However, for many of the applications of interest (Bragg reflectors, planar waveguides etc.) it is unlikely that variation on such a small scale will be significant. In such cases, thickness grown per pulse burst could practically be increased to a few unit cells. It should be noted that significant interdiffusion between garnets (yttrium iron garnet and GGG) has been observed previously for superlattice growth at substrate temperatures of ~ 750 °C and above [8]. While the temperature above which interdiffusion is observed is likely to vary somewhat depending on the materials, high temperatures may prove a tool for smoothing layers via deliberately induced interdiffusion, assuming that growth can still be achieved.

5. Chirped structures

Having achieved simple multilayer growth, more sophisticated structures were fabricated. Chirped structures are of interest ultimately in the context of Bragg reflectors, dispersion compensation etc; however, growth of un-optimized chirped structures proves an effective demonstration of the capabilities of the shutter technique.

These samples were grown using the same setup as the simple multilayers, and again consist of alternating layers of GGG and GSGG. Unlike the simple multilayers, however, the periodicity of the samples varies across the structure. Each chirped structure can be considered as a series of multilayers (“sections”) grown on top of one another. Periodicity of a single section is constant (i.e. layers are of approximately equal thickness) but different from that of other sections. Two configurations were grown:

- **Structure 1: Simple chirp.** Thirteen sections, each consisting of a pair of GGG and GSGG layers. The first section was grown with pulse bursts of 700 shots on each target (i.e. 700 shots per layer); the second with 650 shots per burst, the third with 600 shots per burst and so on in steps of 50, with layers in the final sections grown with 100 shots per burst.
- **Structure 2: Compensated chirp.** Consisting of nine sections, the number of layers in each section was varied as illustrated in Fig. 4, so that each section was grown using ~ 6000 shots in total. This means that each section has approximately equal thickness, and hence scatters an equal contribution of X-rays (ignoring attenuation).

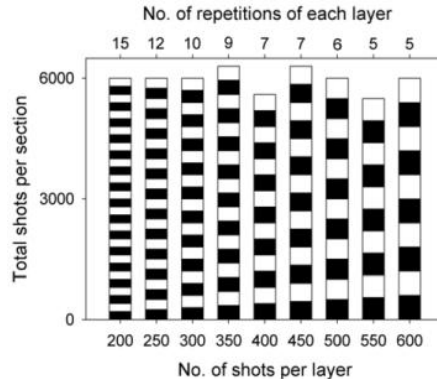


Fig. 4. Diagram showing the number of repetitions of each layer in each component superlattice section within the compensated chirped structure. Layers of GGG and GSGG are represented by black and white areas respectively. The number of layer repetitions is chosen so that the overall thickness of each section is approximately equal (~ 6000 shots in total).

The thickest layers for chirped samples were grown with pulse bursts of 700 shots per layer, corresponding to ~15 nm thick layers. Superlattice XRD pattern behavior is therefore expected and indeed, is observed. Low-resolution XRD spectra for both chirped samples exhibit satellite peaks, and can be considered as a superposition of the individual spectra for each of the component superlattice sections (see Fig. 5). In both cases, structures are crystalline, with the width of central film peaks matching that of the substrate. For the compensated chirp structure (sample 2), there is a greater contribution from each of the components, due to their increased thicknesses. This was as expected, and serves as further proof of the potential for control over the design and growth of more sophisticated structures.

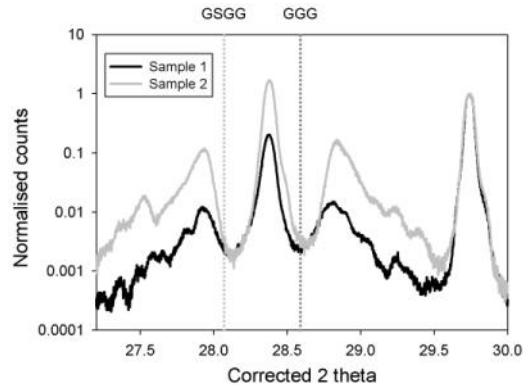


Fig. 5. Low resolution XRD data for two chirped multilayer structures. Sample 1 (simple chirp) is shown in black, sample 2 (compensated chirp) is in grey. Spectra can be considered as a sum of those from each of the component sections, either pairs of layers of varying thickness (sample 1) or stacked superlattices of approximately the same thickness (sample 2). The peak at 29.74 is that of the underlying YAG substrate.

6. Future work

Bragg reflectors are a potentially valuable optical application for crystalline multilayer geometries. At its most basic, a Bragg reflector consists of a series of alternating layers of two materials. The difference in refractive index of these materials is crucial: the greater the contrast, the fewer layers are required to produce a highly reflective structure. GGG and GSGG were the materials chosen for the experiments in this paper due to their similar characteristics (e.g. composition) and growth conditions. However, the refractive index contrast is very small, only around 0.01. A more appropriate choice of materials in the context of a Bragg reflector is GGG and YAG, a material also previously grown successfully via PLD [4]. The refractive index contrast of these materials is much higher, around 0.13, and hence fewer layers (and a smaller overall thickness) are required for a highly reflective structure.

Modeling of such a reflector has been carried out using the *MATLAB* software package; a structure consisting of 58 alternating YAG and GGG layers on a YAG substrate is predicted to result in 90% reflectivity. Similarly, 99% reflectivity is predicted to be achievable with a structure consisting of 90 layers (see Fig. 6). These example structures would have total thicknesses of 8.1 μm and 12.5 μm respectively, excluding substrates.

Modeling assumes bulk values of refractive index, which are not expected to be achieved exactly due to deficient film stoichiometry, and growth conditions common to all materials in the structure must be identified. Despite these issues, however, we anticipate such reflectors being feasible. Given the level of control demonstrated above, more sophisticated designs, including notch and dispersion-compensated reflectors, are very much a possibility.

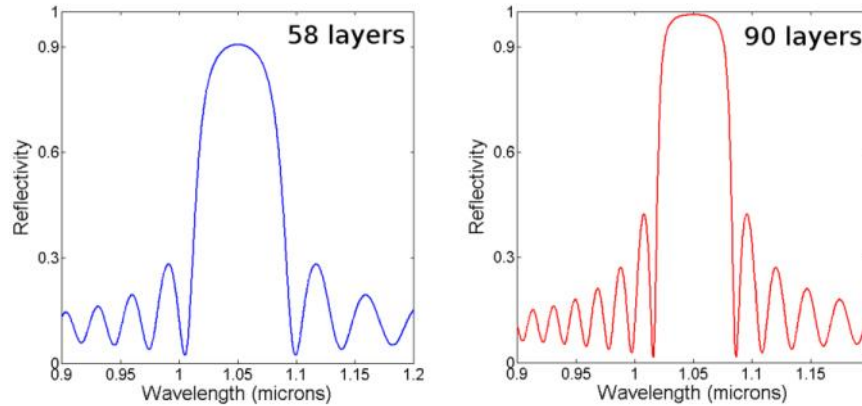


Fig. 6. *MATLAB* simulations suggest that reflective structures of 90% reflectivity and above could be fabricated using 58 layers of YAG and GGG.

7. Conclusions

Crystalline multilayer garnet structures have been fabricated via multi-beam, multi-target PLD in conjunction with a system of mechanical shutters. High-resolution XRD shows three regimes of behavior: mixed layer, superlattice and “true” multilayer in order of layer thickness. Superlattice behavior, and therefore layering, is observed for layer thicknesses of around 2 nm and above. Some layering may also be present at a sub-unit cell level, although this could not be measured. XRD and XRR simulations have been fitted to the experimental data to give material parameters. More sophisticated chirped structures have also been fabricated as proof of principle, opening the way for growth of designer multilayer and graded structures.

Acknowledgements

This work was funded by the Engineering and Physical Sciences Research Council (EPSRC) under grant no. EP/F019300/1. The authors would like to thank Prof. Mark T Weller and Dr Mark E Light for access to X-ray diffraction facilities in the School of Chemistry at the University of Southampton. K. A. Sloyan would like to acknowledge the support of an EPSRC studentship. The Panalytical X’Pert Pro used for the high-resolution X-ray measurements in this research was obtained, through Birmingham Science City: Creating and Characterising Next Generation Advanced Materials, with support from Advantage West Midlands (AWM) and part funded by the European Regional Development Fund (ERDF).